Supplement of Earth Syst. Dynam., 16, 2087–2100, 2025
https://doi.org/10.5194/esd-16-2087-2025-supplement

Earth System Dynamics
Open Access

Supplement of

Conditions for instability in the climate–carbon cycle system

Joseph Clarke et al.

Correspondence to: Joseph Clarke (j.j.clarke@exeter.ac.uk)

Sect. S1 Critical Lambda

Setting equation (12) to zero gives

$$\lambda = \frac{A}{B} \tag{Eq. S1}$$

with

$$\begin{aligned} A = -c_2\nu_1\nu_2 \left(\kappa \log(2) C_A^* \left(\frac{\mathrm{d}\Pi}{\mathrm{d}C_A}\mathcal{E}'\frac{V_1}{V_2}C_L^* + \Pi_0(\mathcal{E}'\frac{V_1}{V_2} + \frac{V_1}{V_2} + 1)\right) - \alpha\beta\mathcal{E}'\Pi_0 Q_{2\times}\frac{V_1}{V_2}C_L^*\right) \\ - c_1\kappa\nu_1\nu_2\log(2)C_A^*\left(\frac{\mathrm{d}\Pi}{\mathrm{d}C_A}\mathcal{E}'\frac{V_1}{V_2}C_L^* + \Pi_0(\mathcal{E}'\frac{V_1}{V_2} + \frac{V_1}{V_2} + 1)\right) \\ + \alpha\beta\kappa\Pi_0 Q_{2\times}C_L^*\left(\mathcal{E}'\nu_1 + \nu_2\left(\frac{V_1}{V_2} + 1\right)\right) \end{aligned} \tag{Eq. S2}$$

and

$$\begin{aligned} \frac{B}{\log(2)C_A^* C_L^*} = \nu_1\left(\nu_2\left(c_2\frac{\mathrm{d}\Pi}{\mathrm{d}C_A}\mathcal{E}'\frac{V_1}{V_2} + \mathcal{E}'\kappa\frac{V_1}{V_2} + \kappa + \kappa\frac{V_1}{V_2}\right) + \frac{\mathrm{d}\Pi}{\mathrm{d}C_A}\mathcal{E}'\kappa\right) \\ + \frac{\mathrm{d}\Pi}{\mathrm{d}C_A}\kappa\nu_2\left(\frac{V_1}{V_2} + 1\right) \\ + \Pi_0\left(\nu_1\left(c_2\nu_2\left(\mathcal{E}'\frac{V_1}{V_2} + \frac{V_1}{V_2} + 1\right) + (\mathcal{E}' + 1)\kappa\right) + \kappa\nu_2\left(\frac{V_1}{V_2} + 1\right)\right) \end{aligned} \tag{Eq. S3}$$

where $\mathcal{E}' = \mathcal{E}'(C_1^*)$ and the prime denotes a derivative with respect to C_1. We can simplify this further by making the 'obvious' assumption that $\mathcal{E}'\nu_1 \gg \nu_2$, $\nu_1 \gg \nu_2$, $c_2 \gg c_1$ and $1 \gg V_1/V_2$. Neglecting these small terms and rearranging gives

$$\frac{\alpha\beta Q_{2\times}}{\lambda \log 2} = \frac{C_A^*}{\kappa\Pi_0 C_L^*\mathcal{E}'\nu_1}\frac{\kappa C_L^*\frac{\mathrm{d}\Pi}{\mathrm{d}C_A}\mathcal{E}'\nu_1 + \kappa C_L^*\nu_1\nu_2 + \Pi_0\left(\kappa\nu_1 + \mathcal{E}'\kappa\nu_1 + c_2\nu_1\nu_2\right)}{1 - \frac{C_A^*\nu_2 c_2}{C_L^*\mathcal{E}'\alpha\beta Q_{2\times}}}. \tag{Eq. S4}$$

Applying the binomial theorem to the denominator and working to first order gives

$$\frac{\alpha\beta Q_{2\times}}{\lambda \log 2} = \left(\frac{\mathrm{d}\log\Pi}{\mathrm{d}\log C_A} + \frac{C_A^*}{C_L^*}\left(1 + \frac{1}{\mathcal{E}'} + \frac{c_2\nu_2}{\kappa\mathcal{E}'} + \frac{C_L^*\nu_2}{\Pi_0\mathcal{E}'}\right)\right)\left(1 + \frac{C_A^*\nu_2 c_2}{C_L^*\mathcal{E}'\alpha\beta Q_{2\times}}\right) \tag{Eq. S5}$$

as desired.

Sect. S2 Fitting *Alk*

The parameter *Alk* was estimated by fitting the ocean model (equation (1d) and equation (1e)) to the ocean carbon uptake from the Global Carbon Budget (GCB) [Fri+22].

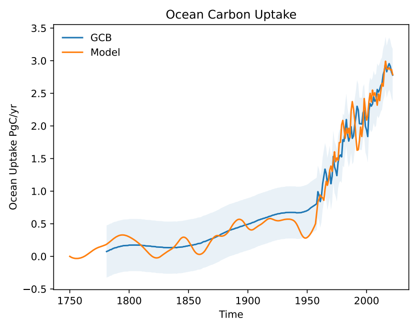

Figure S1: The ocean carbon uptake as estimated by equation (Eq. S6), where *Alk* has been chosen to minimise the squared error between the estimated uptake and the GCB ocean uptake estimate.

The system

$$\frac{\mathrm{d}C_1}{\mathrm{d}t} = \nu_1(C_A(t) - \mathcal{E}(C_1)) - \nu_2\left(C_1 - \frac{V_1}{V_2}C_2\right) \quad \text{(Eq. S6a)}$$

$$\frac{\mathrm{d}C_2}{\mathrm{d}t} = \nu_2\left(C_1 - \frac{V_1}{V_2}C_2\right) \quad \text{(Eq. S6b)}$$

was integrated with $C_A(t)$ defined as the mass of CO_2 in the atmosphere in year t as estimated by GCB. The ocean uptake, defined as the change in $C_1 + C_2$ in each year could then be compared to the annual ocean uptake as estimated by GCB. The parameter *Alk* was chosen to minimise the squared error between these quantities. The best fit parameter of *Alk* was 5130 Pg C.

The fitted ocean carbon uptake is shown in Fig. S1.

Sect. S3 JULES-IMOGEN

Figure S2 shows the response of NPP in JULES to increased CO_2. Atmospheric CO_2 was increased linearly at a rate of 5 ppm yr^{-1} with IMOGEN's climate sensitivity set to 3.3 K. It was found that equation (3) could reproduce the results of this experiment with Π_0 set to 65 Pg C yr^{-1} and $C_{1/2}$ set to 344 ppm.

Figure S3 shows the total soil carbon in JULES after spin up. Over the course of the simulation, the soil carbon changes by 0.008% and has an average of 1630 Pg C.

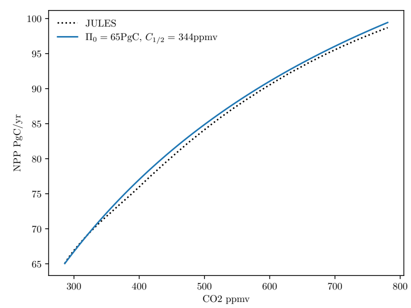

Figure S2: The response of NPP to increased CO_2 in JULES, with a climate sensitivity of 3.3 K. CO_2 was increased linearly by $5\,\mathrm{ppm\,yr}^{-1}$. Equation (3) was linearly regressed to this to give an estimate for $C_{1/2}$. The value of Π_0 was also extracted.

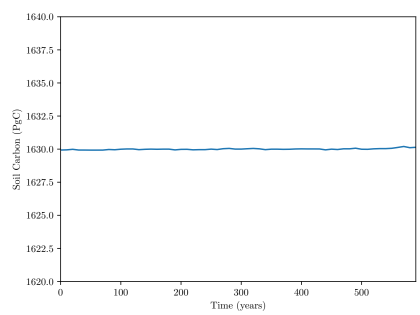

Figure S3: Equilibrium soil carbon. The change is 0.008% over the course of the simulation.

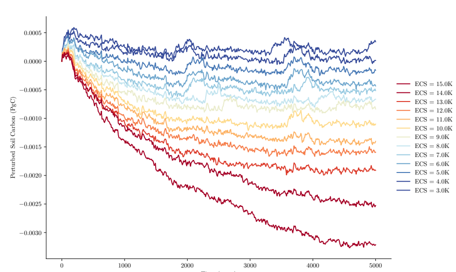

Figure S4: Change in global soil carbon in JULES/IMOGEN for a range of ECS values. The decrease indicates the rise in CO_2 is caused by a loss of soil carbon.

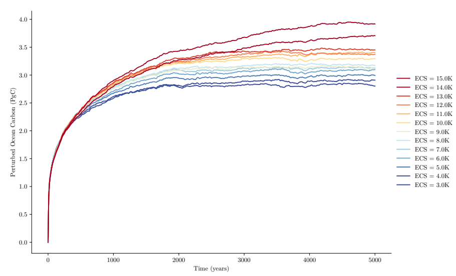

Figure S5: Change in ocean carbon JULES/IMOGEN for a range of ECS values. The rise is caused by absorbing the initial CO_2 perturbation.

References

[Fri+22] Pierre Friedlingstein et al. "Global Carbon Budget 2022". In: *Earth System Science Data* 14.11 (Nov. 2022), pp. 4811–4900. ISSN: 1866-3516. DOI: 10.5194/essd-14-4811-2022. URL: https://essd.copernicus.org/articles/14/4811/2022/.